

## Mineralogy, Geochemistry and Provenance of Kaolins from the Paleolake of Ngaoundere (Cameroon, Central Africa)

<sup>1</sup>Nguetnkam Jean Pierre, <sup>1</sup>Ganwa Alembert Alexandre, <sup>2</sup>Kamga Richard, <sup>3</sup>Ekodeck Georges Emmanuel

<sup>1</sup>Department of Earth Sciences, Faculty of Science,

University of Ngaoundere, P.O. Box 454 Ngaoundere, Cameroon

<sup>2</sup>Department of Applied Chemistry, National High School of Agro Industrial Sciences,

University of Ngaoundere, P.O. Box 455 Ngaoundere, Cameroon

<sup>3</sup>Department of Earth Sciences, Faculty of Science, University of Yaounde I, P.O. Box 812 Yaounde,

**Abstract:** This research deals with mineralogical and geochemical studies of 4 kaolins from paleolake of Ngaoundere in order to investigate their composition (mineralogical composition, distribution of major, trace and rare earth elements) and to assess their source area composition. Methodologies based on the description of outcrops and boreholes, using X-Ray Diffraction (XRD), Diffuse Reflectance Infrared Fourier Transform Spectroscopy (DRIFTS), Transmission Electron Microscopy equipped with an Energy Dispersive X-ray Spectrum (TEM-EDS) and chemical analyses allowed for the definition of 2 main groups of sedimentary kaolins within the paleolake. The first group occurs at the upper part of the paleolake and is characterized by relative high SiO<sub>2</sub> and Al<sub>2</sub>O<sub>3</sub>, High (La/Yb)<sub>N</sub>, (Gd/yb)<sub>N</sub> ratios, high LILE, High La and low TiO<sub>2</sub>, Zr/Th, TTE and HFSE. These data indicate that the above mentioned kaolins were generated from an intense weathering of a granite source and transported and deposited in the actual paleolake. The second group occurs at the lower part of the paleolake and is characterized by relative high TiO<sub>2</sub>, TTE, HFSE, Zr/Th and relative low SiO<sub>2</sub> and Al<sub>2</sub>O<sub>3</sub>, low (La/Yb)<sub>N</sub>, (Gd/yb)<sub>N</sub> ratios, low LILE and low La. These kaolins were generated by an intensive weathering of a mix granite/basalt composition source and also transported and deposited in the actual paleolake. Kaolinite is the predominant phyllosilicate, associated to minor amounts of quartz, goethite, anatase, illite, gibbsite and organic matter. Kaolins of the first group, due to their relative low iron mineral content (< 2.5) could be used in the ceramic industries, paper coating and pain. Industrial use of the kaolins of the second group requires a beneficiation step to remove iron mineral and organic matter.

**Key words:** Kaolin, mineralogy, geochemistry, provenance, paleolake, cameroon

### INTRODUCTION

Kaolins occur widely in many part of Cameroon. Three types can be distinguish in respect with their formation: Primary kaolin formed by meteoric weathering of different rocks (Watong *et al.*, 1996; Ossah, 1975), kaolin formed by hydrothermal weathering (Njoya *et al.*, 2005) and sedimentary kaolin (Thibault and La Bere, 1985; Nguetnkam *et al.*, 2001).

Economic importance of kaolin is well known (Murray, 2000; Harben, 2002), sedimentary kaolins generally having higher economic values than primary kaolins. Until present, the industrial usage of kaolin in Cameroon has been restricted to the manufacturing of bricks, pottery and little on ceramic ware, although works

have been carried out in view of their use in pharmacy and plastic industries (Njopwouo, 1984; Njopwouo *et al.*, 1998).

Because, kaolin genesis has a direct impact on its industrial applications, knowledge on the process of the kaolin genesis and the mineral quality is an important step, prior to technological tests and industrial developments.

The kaolin deposit of the paleolake of Mardock was recently discovered (Nguetnkam *et al.*, 2001) and it is not yet exploited. Further, no detailed study has been carrying out. In this study, analyses on the mineralogy and geochemistry of the kaolin were performed in order to elucidate its origin. Its possible applications in industry are also suggested.

**Corresponding Author:** Nguetnkam Jean Pierre, Department of Earth Sciences, Faculty of Science, University de Ngaoundere, P.O. Box 454 Ngaoundere, Cameroon

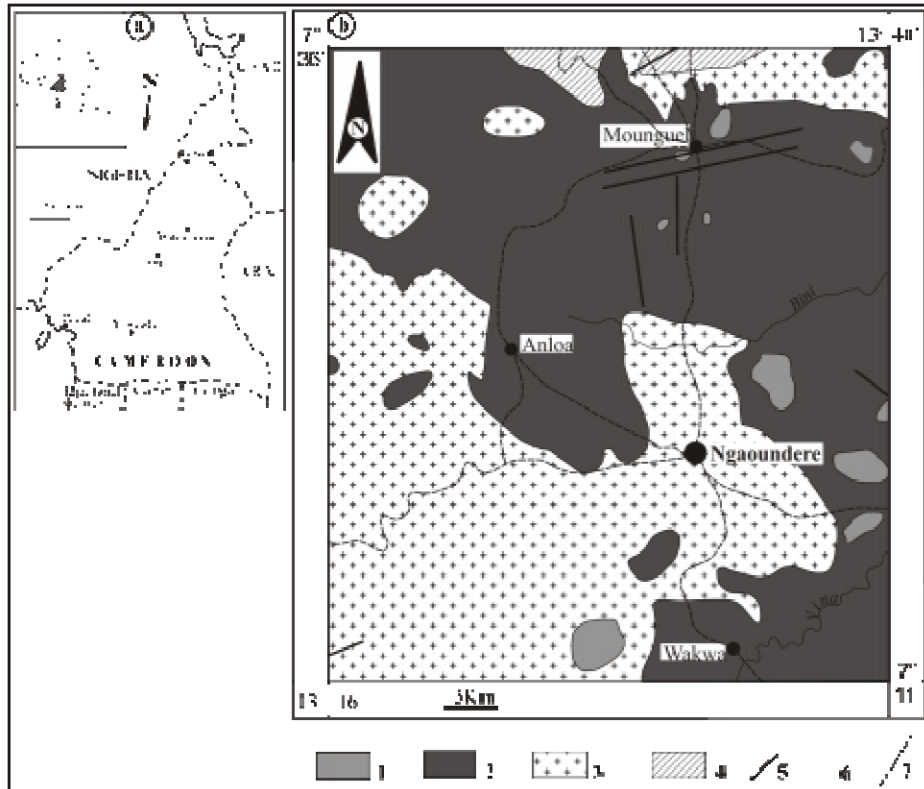


Fig. 1: Map of Cameroon showing the neighbouring country and the main cities. Note the position of Ngaoundere at the centre of the country. CRA: Central Republic of Africa 1b: Geological map of Ngaoundere area. 1: trachyte and phonolite domes; 2: basalts; 3: granites; 4: Gneiss; 5: Fault; 6: Rivers; 7: Roads

**Geological setting and natural environment:** The Adamawa plateau is made up of Pluto-metamorphic basement, crosscut or covers by volcanic formations (Fig. 1).

Metamorphic rocks are constituted of 2.1 Ga gneisses and amphibolites which have been remobilised during Panafrican orogeny (Toteu *et al.*, 2001).

Granitic rocks belong to a large batholith known as Adamawa-Yade massif. They were dated at Ordovician by Regnault (1986). Petrographically, they are constituted of amphibole-biotite granite, biotite-muscovite granite and biotite granite (Tchameni *et al.*, 2006). At the level of Ngaoundere area, the granite was emplaced during late Neoproterozoic (Tchameni *et al.*, 2006); it is crosscut by lower Paleozoic doleritic dyke to the west of the Ngaoundere city (Vicat *et al.*, 2001).

The basement (granites and dolerite) are partially covered by miopliocene volcanic rocks which are constituted of basaltic, phonolitic and trachytic flows (Temdjim, 1986; Ngounouno, 1998)

The Adamawa area is affected by faults, which reactivation during Mesozoic and Cainozoic lead to the formation of the Mbéré and Njerem trenches (Eno Bélinga,

1986; Guiraud and Maurin, 1992). It is an E-W stretching structure at the centre of Cameroon with an average altitude of 1200m. Segalen (1967) and Fritsch (1978) describe the arrangement of plateaus and planes in Cameroon as due to the erosion of Jurassic or cretaceous surfaces. The velocity of this regressive erosion which, from Eocene to Oligocene created the Meiganga surface (1000-1300m, South Adamawa) and Minim-Martap plateau (1400-1700m, West Adamawa), was estimated at 10m/Ma by Tardi and Roquin (1998). Eno Belinga (1986) defines 5 tectono-geomorphologic blocks in Adamawa area with respect to the altitude. The Ngaoundere plateau belongs to the block with altitude of 1000-1200 m. It is dominated by few granitic crowns. The morphology in Cameroon was attributed not only to the erosion, but also to the tectonic with the reactivation of Precambrian faults (Morin, 1989). Therefore, many localities situated today at high altitude are due to the combine action of erosion and tectonic. It is the case in the Ngaoundere city where a paleolake was recently discovered at the top of a plateau at altitude 1110 m (Nguetnkam *et al.*, 2001). This plateau is bordered by rivers (Fig. 2a) and surrounding by plateaux of altitude > 1110m. Located 80 km to the NW of

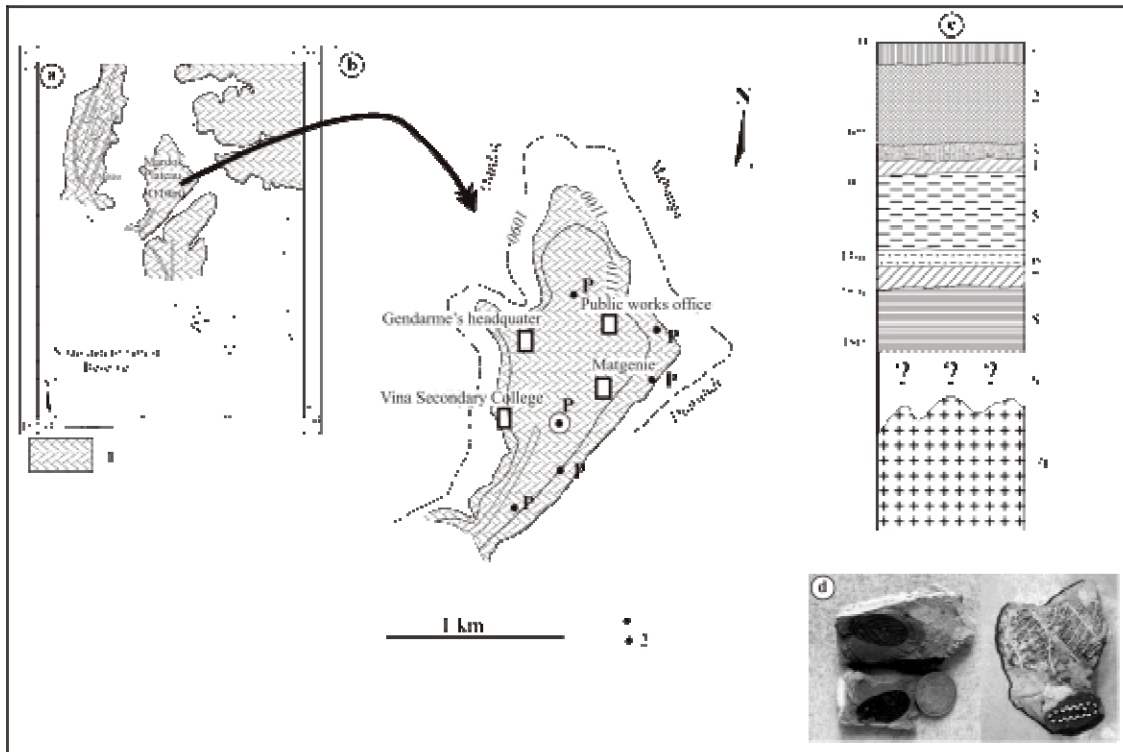


Fig. 2: Map of Ngaoundere showing the plateau (1) to the North of the city, 2b: Map of the Mardock plateau showing the location of the explored Boreholes. 1: main borehole; 2: secondary borehole, 2c: Lithostratigraphy of paleolake of Ngaoundere. (1): brown soft clayey layer; (2): purple massive kaolin (AVMARD); (3): firm brown clay sandy layer; (4): brown yellowish sand clayey layer; (5) white massive kaolin (ABMARD); (6): brown yellowish layer; (7): yellow massive kaolin (AJMARD); (8): grey to dark massive kaolin; (9): unexplored zone; (10) granites, 2d: Fossils impress in the grey to dark kaolin

the Ngaoundere city, the Anloa basin is made up of grey-blue sand, grey to black clay with post mio-pliocene impress fossil of leaf (Salaard-Cheboldaeff *et al.*, 1992).

The actual climate of Ngaoundere is the wet and dry type classified as Tropical rainy climate by Suchel (1987). It is characterized by a mean annual rainfall of 1400 mm, peaking between July and August and a mean annual temperature of 22°C. The study area is covered by the northern Guinea Savanna vegetation zone; but, the native vegetation has been considerably altered by human activities.

**Lithostratigraphy and age of sediments of the paleolake of mardock:** The paleolake of Mardock is located at the north of Ngaoundere, at an altitude of 1110 m, on a plateau bordered by valleys and rivers and surrounding by plateaux of altitude > 1110 m (Fig. 2a,b). Exploration of outcrops and boreholes reveals the lithostraty of this paleo milieu, which shows from the top to the base (Fig. 2c):

- A brown soft clayey layer, 0.85 m;
- A purple massive kaolin (AVMARD): 4, 5-5 m;
- A firm brown clay sandy layer, 0.7 m;
- A brown yellowish sand clayey layer, 0.6 m
- A white massive kaolin (ABMARD): 4 m;
- A brown yellowish layer, 0.8 m
- A yellow massive kaolin (AJMARD): 1,6 m;
- A grey to dark massive kaolin (AGMARD), finely stratified, with well preserved fossil impress of leaves (Fig. 2d): > 3,5 m. Those fossil impress have been identified as leaves belonging to *Combretum collinum* (Combretaceae), *Leptadenia arborea* (Ascepiadaceae), *Sarcocephalus latifolius* and *Terminalia laxiflora*.

The boundary between the eight identified layers is sharp, suggesting that they are genetically discontinuous and are result of different phases of erosion, transport and deposits. The fine lamination observed on the grey to dark kaolin indicates that it was deposited in a quiet aquatic environment. The presence of well preserved fossil impress is also indicative of an undisturbed environment of deposition.

In comparison with sediments of the Anloa basin, located at 80 km to the NW of the Ngaoundere city and on the basis of the regional historical geology, a Pliocene age had been proposed for the sediments of the Ngaoundere paleolake (Nguetnkam *et al.*, 2001).

Ecological exigencies of plants, whose leaves imprints are observed on clays, allow deducing that their paleoenvironment is closed to that of the actual Sudanguinea climate of the Adamawa.

In this study, the 4 facies of kaolin identified within the paleolake are analysed.

### MATERIALS AND METHODS

For laboratory investigations, samples of the 4 facies of kaolin were obtained from the main borehole. They are labelled AVMARD for purple massive kaolin, ABMARD for white massive kaolin, AJMARD for yellow massive kaolin and AGMARD for Gray to dark massive kaolin with fossil impress of leaf.

XRD and DRIFTS were performed at "Laboratoire Environnement et Minéralurgie, ENSG" (Nancy, France). X-Ray Diffraction (XRD) analysis was performed on randomly oriented powder preparation from bulk and on oriented samples from clay fraction, using a D8 Bruker diffractometer with Co  $\alpha_1$  radiation ( $\lambda=1.7891$ ). The clay fraction was extracted by the pipette international method.

Infrared spectra were recorded using an IFS 55 Bruker Fourier Transform IR spectrophotometer equipped with a MCT detector ( $4000-600\text{ cm}^{-1}$ ) cooled at 77K and in diffuse reflectance mode (Harrick attachment). Seventy milligram of clay sample were mixed with 370 mg of KBr. The spectra were recorded by accumulating 200 scan with a  $4.0\text{ cm}^{-1}$  resolution.

Cation Exchange Capacities (CEC) were measured at neutral pH using cobaltihexammonium ions  $[\text{Co}(\text{NH}_3)_6]^{3+}$  as exchangeable probe. The equilibrium pHs of bulk soils suspensions were measured with a standard LPH 330 T electrode.

Chemical analyses were performed on both bulk soil samples at the CRPG (Nancy, France). The major elements were determined by Inductively Coupled Plasma - Atomic Emission Spectroscopy (ICP-AES) while trace elements and rare earths elements were determined by Inductively Coupled Plasma - Mass Spectroscopy (ICP-MS). Relative analytical uncertainties are estimated at 1-2% for major elements. They reach 5% for most of the trace element concentrations except for Cu and Ni (10%). Uncertainty is high ( $> 10\%$ ) for any trace element displaying low concentration ( $< 0.1\%$ ).

TEM observations were carried out with a Philips CM20 microscope equipped with an EDS detector. SEM observations were carried out with a Hitachi 2500 LB Scanning Electron Microscope equipped with a Kevex Delta EDS spectrometer.

### RESULTS

**X-ray diffraction:** Figure 3 presents the XRD patterns of the randomly oriented powder of the 4 kaolins. According to the relative patterns, they all contained kaolinite as the principal mineral (characteristics peaks at  $7.2\text{ \AA}$  and  $3.58\text{ \AA}$ ) associated to weak amounts of quartz, goethite, anatase, gibbsite and mica. Feldspars are revealed by the presence of the peak at  $4.4\text{ \AA}$ . The presence of these accessory minerals varies between samples. Gibbsite and illite are only present in the purple kaolin and in the yellow kaolin, respectively.

A comparison of the intensity of the diffraction lines showed that yellow kaolin is the most richer in kaolinite and that white kaolin is the most richer in quartz, meanwhile purple kaolin contains weak amounts of quartz. Further, the (060) spacing are less than  $1.50\text{ \AA}$  ( $\sim 1.49\text{ \AA}$ ) (Table 1) and are typical of dioctahedral phyllosilicates including kaolinite.

The XRD patterns of the oriented deposits reveal the presence of quartz only in the white kaolin and in the yellow kaolin (Fig. 4). An analysis of the d 001 reflection gives information on the degree of cristallinity of the samples, especially on the stacking defaults along the c-axis. The basal spacing (001) reflections for pure kaolin is  $7.15\text{ \AA}$  (Trunz, 1976; Tchoubar *et al.*, 1982) and increases with decreasing crystallinity. The obtained values for the

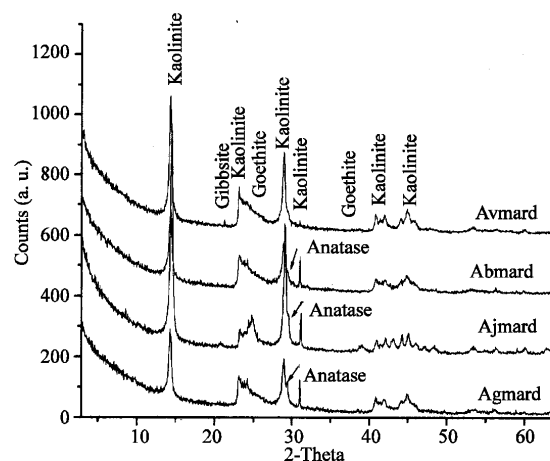


Fig. 3: X-ray diffraction patterns of randomly oriented samples. The vertical scale is shifted by 200, 400 and 600 for samples AJMARD, ABMARD and AVMARD, respectively

Table 1: Basal spacing ( $\text{\AA}$ ), crystallites sizes ( $L_{001}$  and  $L_{002}$ ), pH and CEC of the studied kaolins

Samples	001 line		002 line		060 line	pH	CEC (cmolc kg <sup>-1</sup> )
	$d$ ( $\text{\AA}$ )	$L_{001}$ ( $\text{\AA}$ )	$d$ ( $\text{\AA}$ )	$L_{002}$ ( $\text{\AA}$ )	$d$ ( $\text{\AA}$ )		
AVMARD	7.178	215	3.578	230	1.492	6.6	7.89
ABMARD	7.126	252	3.566	310	1.489	6.5	5.49
AJMARD	7.212	187	3.588	192	1.492	6.6	8.71
AGMARD	7.202	208 ?	3.588	214 ?	1.491	7.2	12.23

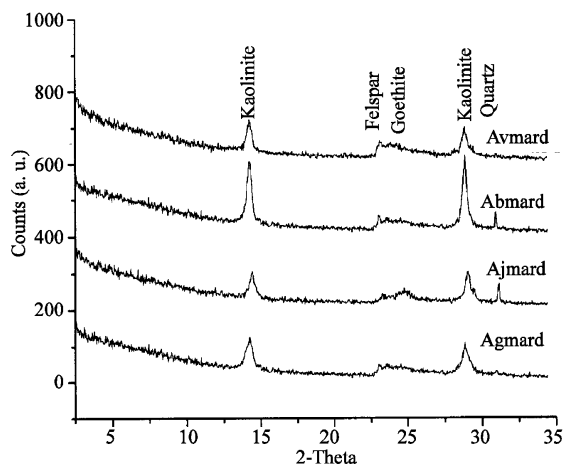


Fig. 4: X-ray diffraction patterns obtained on oriented samples. The vertical scale is shifted by 200, 400 and 600 for samples AJMARD, ABMARD and AVMARD, respectively

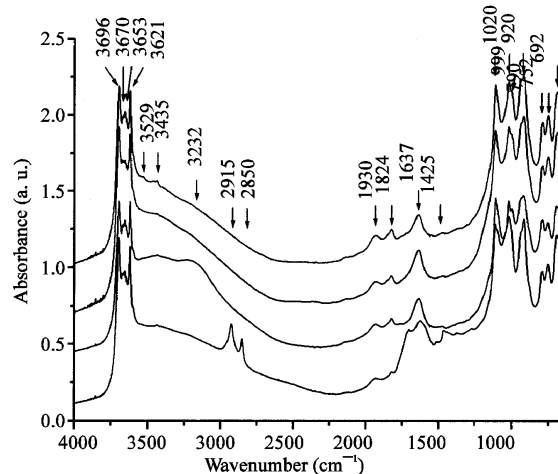


Fig. 5: Infrared spectra obtained on kaolins from paleolake of Mardock. The vertical scale is shifted by 0.3, 0.6 and 0.9, for samples AJMARD, ABMARD and AVMARD, respectively

four studied kaolins are given in Table 1 and indicates that the white kaolin has the highest degree of crystallinity with a basal spacing of 7.126  $\text{\AA}$  and the others have a relative lowest degree of crystallinity, although they are relatively well crystallised. The dimensions of coherent scattering thickness of kaolinite in both facies, which give an assessment of crystallinity, were deduced from the Full-width at Half Maximum (FWHM) by applying Scherrer's equation. Measurements were focused on basal reflections ( $d_{001}$  and  $d_{002}$ ). The values obtained (Table 1) are consistent with the above conclusions concerning the crystallinity of the studied kaolinite. They also show that ABMARD is the most crystalline and AJMARD the less crystalline.

**IR spectroscopy:** The infrared spectra of the studied samples are given in Fig. 5. Globally, all the four kaolins samples display similar spectra feature; they show in the OH-stretching vibrations region (3800-3400  $\text{cm}^{-1}$ ) the four OH stretching bands (3697, 3668, 3653, 3621  $\text{cm}^{-1}$ ) characteristics of kaolinites (Farmer, 1974); and in the 600 - 1200  $\text{cm}^{-1}$  FTIR region, peaks at 1113, 1020, 920, 794 and 693  $\text{cm}^{-1}$ , characteristics of kaolinites. The simultaneous presence of bands at 3668 and 3653  $\text{cm}^{-1}$  suggest the

studied kaolinites have a good crystallinity (Cases *et al.*, 1982; Petit, 1994); this is also confirms by the AlOH bending at 915 and at 937  $\text{cm}^{-1}$  (shoulder).

In the yellow kaolin, the fact that the band at 794  $\text{cm}^{-1}$  is more intense than that at 752  $\text{cm}^{-1}$  confirms the presence of goethite in this sample.

A band at 3529  $\text{cm}^{-1}$  is due to the presence of gibbsite in the purple kaolin and is consistent with XRD results.

Bands at 1825 and 1425  $\text{cm}^{-1}$  suggest the presence of carbonate bearing minerals in all the samples, notably calcite and dolomite.

A band at 3232  $\text{cm}^{-1}$  indicates presence of illite or vermiculite as observed by XRD.

A band at 3435 may be assigned to the OH vibration no well crystallised hydroxyl alumina or to silico alumina gels coating the surface of kaolinite (Delineau, 1994).

The two bands around 2900 indicate the presence of organic matter in the grey kaolin.

The overall results of FTIR are consistent with XRD analyses and further reveal the presence of carbonates bearing mineral and silico alumina gels in all the studied kaolins and the exclusive presence of organic matter in the grey kaolin.

Table 2: Majors elements and trace compositions of kaolins from paleolake of Ngaoundere and of the upper continental crust (Taylor and McLennan, 1985).  
LOI: Loss on ignition; < L.D.: < to detection limits

	AVMARD	ABMARD	AJMARD	MARD AG	UCC
<b>Major elements (g kg<sup>-1</sup>)</b>					
SiO <sub>2</sub>	43.66	44.84	36.31	37.49	65.67
Al <sub>2</sub> O <sub>3</sub>	37.44	35.69	27.72	29.56	15.12
Fe <sub>2</sub> O <sub>3</sub>	2.45	1.56	15.31	1.68	4.98
MnO	< L.D.	< L.D.	< L.D.	< L.D.	0.08
MgO	< L.D.	< L.D.	0.11	0.1	2.19
CaO	< L.D.	< L.D.	< L.D.	< L.D.	4.18
Na <sub>2</sub> O	< L.D.	< L.D.	< L.D.	< L.D.	3.88
K <sub>2</sub> O	0.08	0.15	0.12	0.07	3.38
TiO <sub>2</sub>	1.1	1.25	2.67	2.79	0.5
P <sub>2</sub> O <sub>5</sub>	0.1	0.11	0.33	0.15	---
LOI	15.56	16.15	17.58	28	---
Total	100.39	99.75	100.15	99.84	
<b>Trace elements (mg kg<sup>-1</sup>)</b>					
V	43.16	72.47	188.8	222	60
Cr	89.73	80.23	309.4	111	35
Co	2.957	2.737	3.044	41.94	10
Cu	10.37	6.803	36.58	36.27	---
Ni	28.84	19.56	22.87	88.6	20
Rb	10.02	17.08	13.9	12.63	112
Cs	0.69	0.878	0.689	0.792	3.7
Ba	140.1	235.6	96.19	137.8	550
Sr	77	107.3	47.23	59.77	350
Th	58.99	76.63	61.98	54.03	10.7
U	10.29	5.348	14.02	9.024	2.8
Y	14.65	25.02	29.4	87.96	22.2
Zr	217.8	294.3	561.8	469.5	190
Nb	48.18	48.17	88.61	84.5	25
Hf	6.712	8.75	16.7	11.28	5.8
<b>Rare earth elements (ppm)</b>					
La	131.6	147.7	97.18	114.5	30
Ce	166	206.8	107.2	255.7	64
Pr	23.5	28.41	16.17	32.3	7.1
Nd	73.22	92.04	47.23	131.8	26
Sm	9.91	13.57	6.55	26.56	4.5
Eu	1.772	2.573	1.182	6.168	0.88
Gd	5.296	8.612	4.655	21.1	3.8
Tb	0.748	1.202	0.778	3.109	0.64
Dy	3.701	5.925	4.545	17.16	3.5
Ho	0.575	0.977	0.927	3.124	0.8
Er	1.596	2.519	2.922	8.42	2.3
Tm	0.206	0.347	0.454	1.218	0.33
Yb	1.273	2.183	3.256	8.02	2.22
Lu	0.2	0.31	0.505	1.174	0.32
LREE	406.002	491.093	275.512	567.028	132.48
HREE	13.595	22.075	18.042	63.325	13.91
ΣREE	419.597	513.168	293.554	630.353	146.39

**pH and CEC:** The pH values (Table 1) of the studied kaolins are slightly acidic to neutral (6.5 - 7.2); they reflect the presence of dissolved carbonates as observed with DRIFTS. High pH values (> 6.5 for kaolinite) are indicative of the presence of soluble salts, which may cause problems in many applications (Murray, 1988, 1991).

The CEC values obtained are between 5 and 15 cmol<sub>c</sub> kg<sup>-1</sup> (Table 1); the grey and the yellow kaolins having the highest values, meanwhile the well crystallised white kaolin has the lowest CEC. This may be due to the presence of organic matter and goethite in the grey and yellow kaolins, respectively.

**Geochemistry:** Geochemical composition of the studied materials is listed in Table 2 and compared to that of the Upper Continental Crust (UCC) (Taylor and McLennan, 1985).

**Major elements:** The chemical data correlate with the mineralogical composition and the silica and alumina contents agree with the quartz and kaolinite contents. SiO<sub>2</sub> in the studied samples varies from 36- 44% and Al<sub>2</sub>O<sub>3</sub> from 27-37%, reflecting their high kaolinite content and their low quartz content. Globally, the main oxides are SiO<sub>2</sub>, Al<sub>2</sub>O<sub>3</sub>, Fe<sub>2</sub>O<sub>3</sub> and TiO<sub>2</sub>, whereas MgO, K<sub>2</sub>O and P<sub>2</sub>O<sub>5</sub>

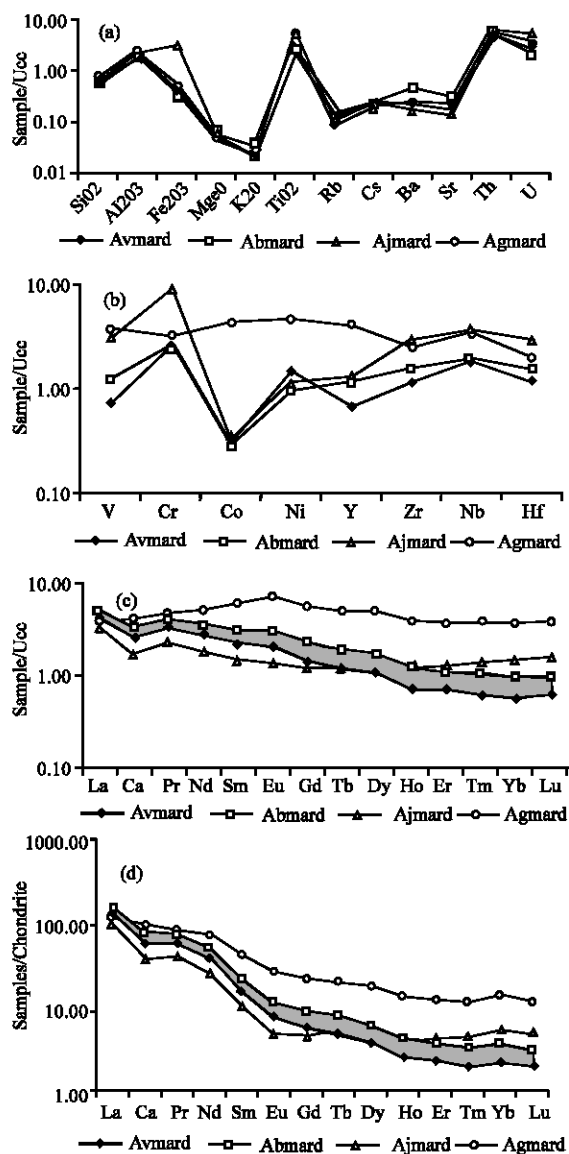


Fig. 6: Compositions of studied kaolins normalized to Upper Continental Crust (UCC, Taylor and McLennan, 1985) and to Chondrite (McDonough and Sun, 1995), 6a: Major and large lithophile elements, 6b: Transition trace and high field strength elements, 6c: rare earth elements normalized to UCC, 6d: rare earth elements normalized to Chondrite

are present only in small amounts. MnO, CaO, Na<sub>2</sub>O and P<sub>2</sub>O<sub>5</sub> are under the detection limit (Table 2). The white kaolin and the purple kaolin have higher amounts of SiO<sub>2</sub> and Al<sub>2</sub>O<sub>3</sub> than the two others kaolins (AJMARD and AGMARD). The concentrations of Fe<sub>2</sub>O<sub>3</sub> vary between 1.55 and 15.33%, with the yellow kaolin having the highest amount.

Yellow clay and grey clay contained a rather large amount of titanium (2.5 < TiO<sub>2</sub> < 3) due probably to the presence of anatase detected by X-ray diffraction. There could also be some structural titanium following substitution of aluminium in kaolinite (Jepson and Rowse, 1975; Sei *et al.*, 2006)

The Loss on Ignition (LOI) varies between 15.56 and 28 and is relatively higher for AJMARD and ABMARD (>17%) than for AVMARD and ABMARD. The highest value obtained in the grey kaolin (28) is probably due to the presence of organic matter.

**The SiO<sub>2</sub>/Al<sub>2</sub>O<sub>3</sub> ratio of all the kaolin is ~ 2 and the SiO<sub>2</sub>/(Fe<sub>2</sub>O<sub>3</sub> + Al<sub>2</sub>O<sub>3</sub>) varies between 1.6 and 2:** Large lithophile elements (LILE): Rb, Cs, Ba, Sr, Th and U In comparison with UCC (Fig. 6a), all studied kaolins are depleted in Rb, Cs, Ba, Sr and enriched in Th and U. Thus, Th and U are positively correlate to Al<sub>2</sub>O<sub>3</sub> and Ti, indicating a similar geochemical behaviour; Rb, Cs, Ba, Sr are positively correlate to others majors elements which display depletion. These observations suggest that Th and U may be controlled by Ti bearing phases associated to kaolinite.

ABMARD and AVMARD are the most enriched in LILE in comparison with the two others studied kaolins (AJMARD and AGMARD).

**High field strength elements (HFSE): Y, Zr, Nb and Hf:** AJMARD and AGMARD are more enriched in HFSE than ABMARD and AVMARD. Nevertheless, the UCC normalized data show that all studied kaolins are enriched in HFSE (Fig. 6b). Thus HFSE show a positive correlation with Th and U and with Al<sub>2</sub>O<sub>3</sub> and TiO<sub>2</sub>. Moreover, Zr/Al<sub>2</sub>O<sub>3</sub> and HFSE/Al<sub>2</sub>O<sub>3</sub> ratio are lower in AVMARD and AJMARD (< 10) and higher in AJMARD and AGMARD (> 15), suggesting that other phases, in addition to kaolinite, are probably hosting HFSE (e.g. iron oxides, Ti-bearing oxide and organic matter).

**Transition trace elements (TTE): V, Cr, Co, Cu and Ni:** Here again, AJMARD and AGMARD are the most enriched in TTE in comparison with ABMARD and AVMARD. However, it should be noted that all kaolins are enriched in TTE relative to UCC. Thus there is a positive correlation between TTE and Al, Ti, Th and U. This observation also suggests that TTE are controlled by kaolinite associate to Ti-bearing mineral (anatase).

**Rare Earth Elements (REE):** To quantify the degree of HREE/LREE fractionation, normalized La/Yb ratio labelled (La/Yb)<sub>N</sub> have been calculated. The (La/Yb)<sub>N</sub> ratios for the four kaolins are between 8.6 and 62.8 (Table 2). AVMARD and ABMARD show (La/Yb)<sub>N</sub> ratios of 62.8 and 41.1,

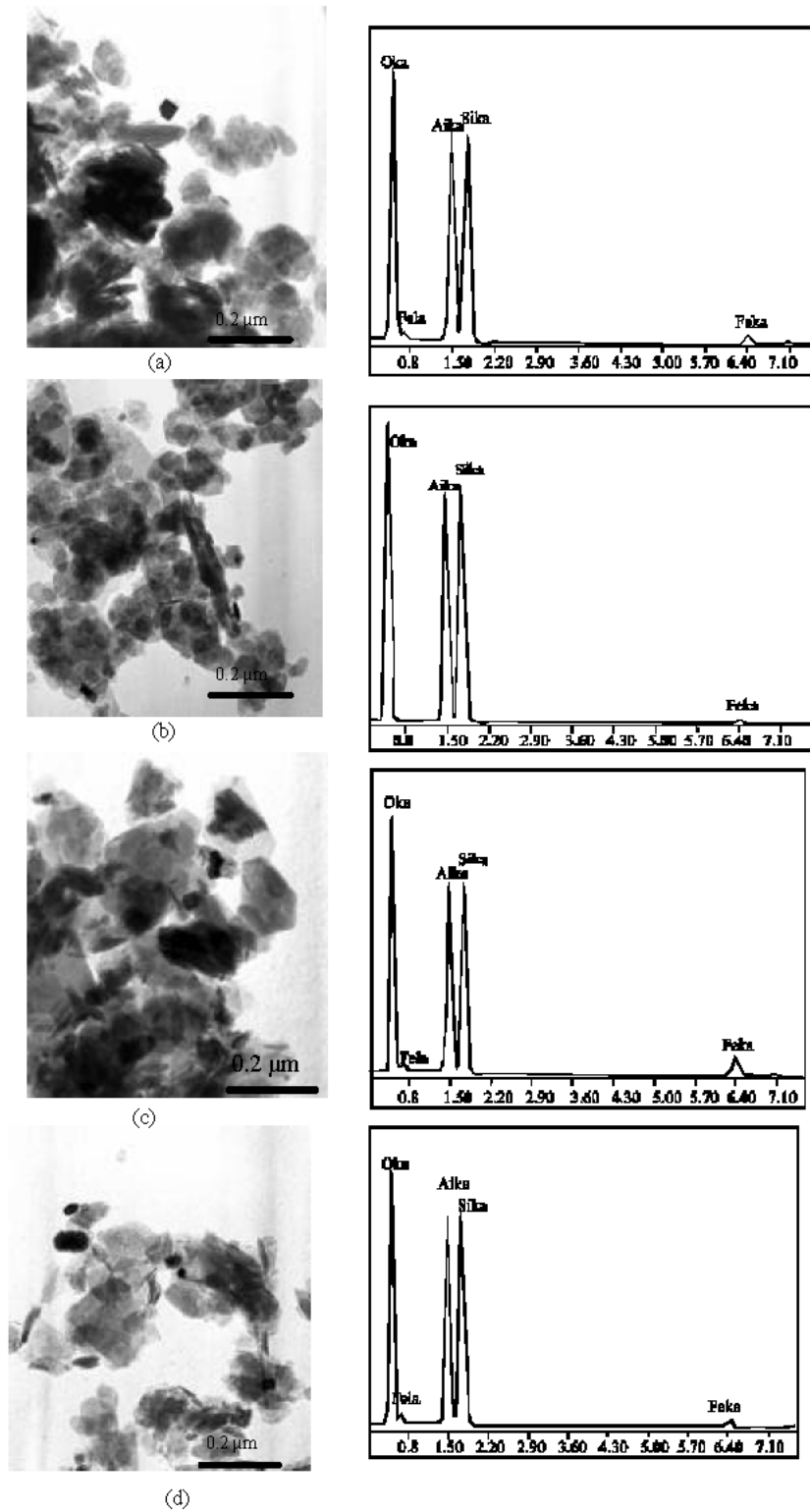


Fig. 7: TEM photograph showing morphology of the studied kaolins and their EDS composition. (a): VMARD, (b): ABMARD, (c): AJMARD, (d): AGMARD



respectively and consequently a strong depletion in HREE and an LREE enrichment. For AJMARD and AGMARD, the  $(La/Yb)_N$  ratios are 18.1 and 8.6, indicating that these samples are richer in HREE. The low  $(La/Yb)_N$  values for these two kaolins make the differentiation between them and the two other kaolins (AVMARD and ABMARD); this let to distinguish two groups: a group with high  $(La/Yb)_N$  values (AVMARD and ABMARD) and a group with low  $(La/Yb)_N$  values (AJMARD and AGMARD).

Further, the  $(Gd/Yb)_N$  ratios are relatively higher ( $>2$ ) in AVMARD and ABMARD than in AJMARD and AGMARD ( $< 2$ ). Conversely, the Zr/Th ratios are relatively lower in AVMARD and ABMARD (3.6 - 3.8), than in AJMARD and ABMARD (8.6 - 9.0), reflecting strong geochemical similarity between AJMARD and AGMARD and between ABMARD and AVMARD.

Moreover, when comparing the REE patterns normalized to UCC of the four kaolins (Fig. 6c), a great similarity is also noted between AVMARD and ABMARD and between AJMARD and AGMARD, although they display globally the same patterns. Likewise, the REE distribution graph normalized to chondrite show the same trend (Fig. 6d).

**Crystal morphology and microchemistry:** TEM observations reveal that the morphology of particles consist in general on irregular platelets well developed and booklets of kaolinite. Pseudo hexagonal structure with angular edges is observed in ABMARD and AJMARD and less in the AVMARD (Fig. 7). Meanwhile, in the AGMARD, platelets with rounded semi hexagonal to irregular edges are observed. In the AJMARD and AVMARD, kaolinite particles are associated to iron oxides particles (goethite), as observed with XRD results.

Elemental composition detected by EDX reveals the presence of O, Al, Si. In addition, EDX spectra of the four samples indicate the presence of Fe which may exist as structural iron or as thin coating on the kaolinite crystals. As one can observe, the EDX analysis indicates Al and Si in an almost equal intensity and O one and a third high than the intensity of the former elements (Fig. 7). The fact that the EDX analysis does not reveal the presence of Ti, suggests that  $TiO_2$  may occur as separate phase, not associated to kaolinite.

## DISCUSSION

**Area source composition:** Geochemical data could potentially be a source of information to determine provenance. For example, REE are useful indicators for provenance characterization, because they are among the

least soluble elements and are usually transported almost exclusively in the terrigenous component of sediment and therefore reflect the chemistry of the source (McLennan *et al.*, 1980; Rollinson, 1993; Lopez *et al.*, 2005). La is more abundant in silicic rocks than in basic rocks and the opposite is true for Co, Cr. Therefore, La/Co, La/Cr ratios may be useful for provenance determinations (Taylor and McLennan, 1985), so that relative enrichment of incompatible over compatible elements (e.g. LREE, High La/Co) indicate an average silicic provenance (McLennan *et al.*, 1993; Cullers and Berendsen, 1998). In addition, basic rocks show less fractionated chondrite-normalized patterns with low LREE/HREE ratio; whereas acidic rocks usually show high fractionated chondrite-normalized patterns (Cullers and Graf, 1983; Taylor and McLennan, 1985) and these patterns have generally been preserved in the sedimentary environment (Taylor and McLennan, 1985; Cullers and Podkovyrov, 2002; Slack and Stevens, 1994).

Geochemical data of the analysed samples reveal that the four kaolins can be classified in 2 groups (Table 3):

A group 1 constituted by AVMARD and ABMARD. These two kaolins are characterized by relative high  $SiO_2$  and  $Al_2O_3$ , High  $(La/Yb)_N$ ,  $(Gd/Yb)_N$  ratios, high LILE, High La and low  $TiO_2$ , Co, Cr, Zr/Th, TTE and HFSE (Table 2 and 3). These geochemical trends suggest that the original source area was predominantly silicic in composition.

A group 2 constituted by AJMARD and AGMARD which display an opposite trend, in comparison with kaolins of group 1: low  $SiO_2$  and  $Al_2O_3$ , low  $(La/Yb)_N$ ,  $(Gd/Yb)_N$  ratios, low LILE and low La and high  $TiO_2$ , Co, Cr, Zr/Th, TTE and HFSE (Table 2 and 3).

Therefore, the above geochemical trend suggests that their original source was predominantly basic in composition or at least has some basic characters. Since, in the studied area, rocks consist mainly of granite and basalt, one can conclude that kaolins of group 1 have been generated from intense weathering of granite, meanwhile those of group 2 derived from weathering of basalt.

In  $TiO_2/Al_2O_3$  diagram (Fig. 8), AVMARD and ABMARD are plotted in the field corresponding to Ryolite/Granite composition, whereas AVMARD and AGMARD are plotted in the field corresponding to Ryolite/Granite + Basalte mix composition. This observation corroborates the above conclusions. The basic character of the source area for AJMARD and AJMARD is confirm in the  $TiO_2/Al_2O_3$  diagram, as also observed with REE and trace elements compositions.

**Paleoweathering conditions:** To determine the degree of source area weathering, the Chemical Index of Alteration

Table 3: Difference between the geochemical characters of the two groups of sedimentary kaolins

	Group 1		Group 2	
	AVMARD	ABMARD	AJMARD	AGMARD
SiO <sub>2</sub> (g kg <sup>-1</sup> )	43.66	44.84	36.31	37.49
Al <sub>2</sub> O <sub>3</sub> (g kg <sup>-1</sup> )	37.44	35.69	27.72	29.56
TiO <sub>2</sub> (g kg <sup>-1</sup> )	1.1	1.25	2.67	2.79
La (mg kg <sup>-1</sup> )	131.6	147.7	97.18	114.5
Cr (mg kg <sup>-1</sup> )	89.73	80.23	309.4	111
Co (mg kg <sup>-1</sup> )	2.95	2.73	3.04	41.94
V (mg kg <sup>-1</sup> )	43.16	72.47	188.8	222
(La/Yb)N	62.86	41.14	18.15	8.68
(Gd/Yb)N	2.52	2.39	0.87	1.60
Zr/Th	3.69	3.84	9.06	8.68
Zr/Al <sub>2</sub> O <sub>3</sub>	5.82	8.25	20.27	15.88
HFSE/Al <sub>2</sub> O <sub>3</sub>	7.67	10.54	25.27	15.88
La/Co	44.50	53.96	31.92	2.7
La/Cr	1.46	1.84	0.31	1.03

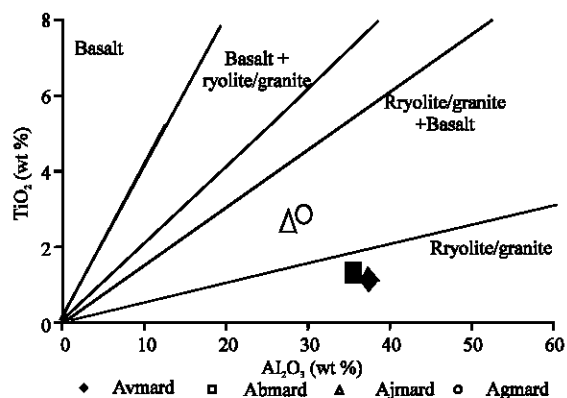


Fig. 8: TiO<sub>2</sub>/Al<sub>2</sub>O<sub>3</sub> binary plot of kaolins from the paleolake of mardock

(CIA, Nesbitt and Young, 1982) and the Mineralogical Index of Alteration (MIA, Voicu and Bardoux, 2002) have been calculated, using the following equations:

$$CIA = [Al_2O_3 / (Al_2O_3 + CaO + Na_2O + K_2O)] \times 100 \quad (1)$$

Where oxides are in molecular proportions

$$\text{and } MIA = 2 \times (CIA - 50) \quad (2)$$

The CIA represents the degree of alteration of feldspars to clay mineral in the course of meteoric weathering. Values from unweathered igneous rocks are about 50, whereas intensively weathered residual rocks forming kaolinite and gibbsite can approach 100.

The MIA value indicates incipient (0-20%), weak (20-40%), moderate (40-60%) and intense to extreme (60-100) weathering. The value of 100% means complete transformation of a primary mineral into its equivalent weathered product and, by extrapolation, complete weathering of the parent rock.

CIA and MIA values of the analysed samples are higher than value of UCC and approach 100% (> 90%). Therefore high CIA and MIA values suggest that these kaolins were generated from an intensively weathered source area. If the chemical weathering was very intense it would imply specific conditions in the source area analogous to that prevailing nowadays in humid tropical regions. In these regions, intense weathering resulted in development of 1:1 phyllosilicates which show a low cation exchange capacity, including kaolinite.

This deduction is supported by the mineralogical data. In fact from XRD analysis and TEM observations, the major component of the studied samples was kaolinite associated to minor amounts of quartz, gibbsite, iron-oxides mineral (goethite) and anatase. These compositions are typical of clays from humid tropical regions.

The high REE content in all the samples in comparison to UCC also suggests a great degree of chemical weathering, in the source area. In fact it is well known that REE are relatively immobile during the sedimentary process and that they are transferred almost quantitatively to sedimentary basin on the particulate matter (McLennan *et al.*, 1980, Taylor and McLennan, 1985; Wronkiewicz and Condie, 1987; Rollinson, 1993).

**Possible applications:** Kaolin have many different applications as reviewed in the literature (Murray, 2000, Harben, 2002), e.g. in the study, paint, rubber, ceramic, plastic, pharmaceuticals and cosmetic industries. Further, brick and pottery industries as well as chinaware and porcelain are very promising application of any mined deposit (Ekosse, 2000).

AVMARD and ABMARD, kaolins of group 1, display low iron content (< 2.5). Therefore, they are suitable raw materials for white burning industrial clays (Murray, 2000).

AGMARD, kaolin of group 2, shows also low iron content and could be used also for white burning

industrial clays. But the presence of organic matter it a disadvantage and a beneficiation process would be required to remove it.

The high iron content of AJMARD (15 %), kaolin of group 2, makes this material unsuitable for the paper industry and others fields where whiteness is required. However it may be used for numerous others applications. Technology tests for industrial suitabilities are still necessary and will be further carried out.

### CONCLUSION

The principal aim of this study was to characterize the kaolin deposit of the paleolake of Mardock in relation with its genesis and possible applications. It comprises four facies of kaolin which display purple, white, yellow and dark grey colour, with a total thickness of more than 15 meters. Kaolinite is the predominant phyllosilicate occurring on both facies. Others minerals associated with the deposit are quartz, feldspar, gibbsite and goethite.

Results of trace elements geochemistry suggest that these kaolins were mainly eroded from a highly weathered area developed from granite or granite/basalt mix composition, transported and deposited in lake, they are sedimentary kaolins.

From mineralogical and chemical composition, the white facies can be considered for white burning industrial clays. Others facies could be exploited in the ceramic sector if well treated, especially considering the high iron content and the organic content.

### REFERENCES

- Cases, J.M., O. Lietard, J. Yvon and J.F. Delon, 1982. Étude des propriétés cristallographiques, morphologiques, superficielles des kaolinites désordonnées. *Bull. Minéralogie*, 105: 439-455.
- Cullers, R.L. and V.N. Podkovyrov, 2002. The source and origin of terrigenous sedimentary rocks in the Mesoproterozoic Uj group, Southeastern Russia. *Precambrian Res.*, 111: 157-183.
- Cullers, R.L. and J. Graf, 1983. Rare Earth Elements in Igneous Rocks of the Continental Crust: Intermediate and Silicic Rocks, Ore Petrogenesis. In: Henderson, P. (Ed.), *Rare-Earth Geochemistry*, Elsevier, Amsterdam, pp: 275-312.
- Cullers, R.L. and P. Berendsen, 1998. The provenance and variation of sandstone associated with the Mid-continent Rift System. USA. *Eur. J. Mineral.*, 10: 987-1002.
- Delineau, T., 1994. Les argiles kaoliniques du Bassin de Charentes (France): Analyses typologique, cristallographique, spéciation du fer et applications. These INPL Nancy, pp: 595.
- Ekosse, G., 2000. The Makoro kaolin deposit, Southeastern Botswana: its genesis and possible industrial applications. *Appl. Clay Sci.*, 16: 301-320.
- Ekosse, G., 2001. Provenance of the Kgwakgwe kaolin deposit in Southeastern Botswana and its possible utilization. *Applied Clay Sci.*, 16: 301-320.
- Eno Belinga, S.M., 1986. Il y a 600 millions d'années... Paléoclimats et métaux, non métaux et substances minérales utiles du Cameroun. Alitaf, Yaoundé, pp: 128.
- Farmer, V.C., 1974. *The infrared Spectra of Minerals*. Miner. Soci., London.
- Fritsch, P., 1978. Chronologie relative des formations cuirassées et analyse géographique des facteurs de cuirassement au Cameroun. *Trav. Doc. CEGET, Bordeaux*, 33: 115-132.
- Guiraud, R. and J.C. Maurin, 1992. Early Cretaceous rifts of western and Central Africa: an overview. *Tectonophysics*, 213: 153-168.
- Harben, P.W., 2002. *The industrial mineral handy book-A guide to markets specifications and prices*. (4th Edn.), Industrial Minerals Information Services, Worcester Park, UK, p: 412.
- Jepson, W.B. and J.B. Rowse, 1975. The composition of kaolinite-An electron microscope microprobe study. *Clays and Clay Minerals*, 45: 310-317.
- Lopez, J.M.G., B. Bauluz, C. Fernandez-Nieto and A.Y. Oliete, 2005. Factors controlling the trace-element distribution in fine-grained rocks: The Albian kaolinite-rich deposits of the Oliete Basin (NE Spain). *Chem. Geol.*, 214: 1-19.
- McDonough, W.F. and S.S. Sun, 1995. The composition of the earth. *Chem. Geol.*, 120: 223-225.
- McLennan, S.M., S.R. Hemming, D.K. McDaniel and G.N. Hanson, 1993. Geochemical Approaches to Sedimentation, Provenance and Tectonics. In: Johnson, M.J., basu, A. (Eds.), *Processes Controlling The composition of Classic Sediments*, Spec. Pap. Geol. Soc. Am., 284: 21-40.
- McLennan, S.M., W.B. Nancy and R. Taylor, 1980. Rare earth element-thorium correlations in sedimentary rocks and the composition of the continental crust. *Geochim. Cosmochim. Acta*, 44: 1833-1839.
- Morin, S., 1989. Hautes terres et bassins de l'Ouest Cameroun. Etude géomorphologique. Thèse Univ. Bordeaux III, pp: 1190.
- Murray, H.H., 1988. World kaolins-diverse quality needs permit different resource types. Proc. 8th Ind. U.S. Minerals Int. Congress. Metal Bull, London, pp: 127-130.
- Murray, H.H., 1991. Overview-clay minerals applications. *Applied Clay Sci.*, 5: 379-395.

- Murray, H.H., 2000. Traditional and new applications for kaolin, smectite, palygorskite: A general overview. *Applied Clay Sci.*, 17: 207-221.
- Nesbitt, H.W. and G.M. Young, 1982. Early Proterozoic climate and plate motions inferred from major element chemistry of lutites. *Nature*, 299: 715-717.
- Ngounouno, I., 1998. Chronologie, pétrologie, et cadre géodynamique du magmatisme cénozoïque de la ligne du Cameroun. Collection Géocam. Press. Univ. Yaoundé 1: 169-184.
- Nguetnkam, J.P., A.A. Ganwa, R. Tchameni and J.B. Tchatchueng, 2001. De l'existence d'un paléolac dans la ville de Ngaoundéré (Cameroun). *Ann. FALSH. Univ. Ngaoundéré*, 6: 47-55.
- Njopwouo, D., 1984. Minéralogie et physico-chimie des argiles de Bomkoul et de Balengou (Cameroun). Utilisation dans la polymérisation du styrène et dans le renforcement du caoutchouc naturel. Thèse Doct. D'Etat, Univ. Yaoundé, Cameroun.
- Njopwouo, D., E. Tèjiogap, F. Sondag, B. Volkoff and R. Wandji, 1998. Caractérisation minéralogique des argiles kaoliniques consommées par géophagie au Cameroun. *Ann. Fac. Sci., Univ. Ydé I*, 31: 319-334.
- Njoya, A., C. Nkoumbou, C. Grosbois, D. Njopwouo, D. Njoya, A. Courtin-Nomade, J. Yvon and F. Martin, 2005. Genesis of Mayouom kaolin deposit (Western Cameroon). *Applied Clay Sci.*, 32: 125-140.
- Ossah, N.H., 1975. Altération des roches volcaniques dans les monts Bamenda, Cameroun. Géologie, minéralogie et géochimie. Thèse Doct. 3<sup>ème</sup> cycle, Univ. Paris VI, France.
- Petit, S., 1994. Hétérogénéité et variabilité de la composition des minéraux argileux: À quelle échelle? Discussion de la notion de solution solide. HDR, Univ., poitiers, France.
- Regnault, J.M., 1986. Synthèse géologique du Cameroun. Min. Mines et Energ., Rép. Cameroun, pp: 119.
- Rollinson, H.R., 1993. Using geochemical data: Evaluation, Presentation, Interpretation. Longman, pp: 352.
- Salard-Chebouldaerff, M., J. Mouton and M. Brunet, 1992. Paléoflore tertiaire du Bassin d'Anloua, plateau de l'Adamaoua, Cameroun. *Revista Española de Micropaleontologia*. 14: 131-162.
- Segalen, P., 1967. Les sols et la géomorphologie du Cameroun. Cah. ORSTOM, Paris, Sér. Pédol., 2: 137-187.
- Sei, J., F. Morato, G. Kra, S. Staunton, H. Quiquampoix, J.C. Jumas and J. Olivier-Fourcade, 2006. Mineralogical, crystallographic and morphological characteristics of natural kaolins from the Ivory Coast (West Africa). *J. Afr. Earth Sci.*, 46: 245-252.
- Slack, J.F. and P.J. Stevens, 1994. Classic metasediments of the Early proterozoic Broken Hill Group, New South Wales, Australia: geochemistry, provenance and metallogenic significance. *Geochim. Cosmochim. Acta*, 58: 3633-3652.
- Suchel, J.B. 1987. Les climats du Cameroun (Climates of Cameroon). Tome III. Thèse Univ. St. Etienne, pp: 1186.
- Tardi, Y. and C. Roquin, 1998. Dérive des continents, Paléoclimats et altérations tropicales. (Ed.) BRGM, pp: 473.
- Taylor, S.R., S.M. McLennan, 1985. The Continental Crust: Its Composition and Evolution. Blackwell, Oxford, pp: 312.
- Tchameni, R., A. Pouclet, J. Penaye, A.A. Ganwa and S.F. Toteu, 2006. Petrography and geochemistry of Ngaoundere Pan-African granitoids in central North Cameroon: Implications for their sources and geological setting. *J. Afr. Earth Sci.*, 44: 511-529.
- Tchoubar, B., A. Plançon, J. Ben Brahim, C. Clinard and C. Sow, 1982. Caractéristiques structurales des kaolinites désordonnées. *Bull. Minéralogie*, 105: 477-491.
- Temdjim R., 1986. Le volcanisme de la région de Ngaoundéré (Adamaoua-Cameroun). Etude volcanologique et pétrographique. Thèse 3<sup>ème</sup> cycle Univ. Clermont Ferrand, pp: 185.
- Thibault, P.M. and P. Le Bere, 1985. Les argiles pour brique. B.R.G.M. CRMO, MIMEE, Yaoundé, Cameroun, pp: 65.
- Toteu S.F., W.R. Van Schmus, J. Penaye and A. Michard, 2001. New U-Pb and Sm-Nd data from north-central Cameroon and its bearing on the Pre-Pan African history of central Africa. *Precamb. Res.*, 67: 321-347.
- Trunz V., 1976. Influence of crystallite on the apparent basal spacings of kaolinite. *Clays and Clay Minerals*, 24: 84-87.
- Vicat, J.P., I. Ngounouno and A. Pouclet, 2001. Existence de dykes doléritiques anciens à composition de tholéiites continentales au sein de la province alcaline de la ligne du Cameroun. Implication sur le contexte géodynamique. *C.R.Acad. Sci.*, 332: 243-249.
- Voicu, G. and M. Bardoux, 2002. Geochemical behaviour under tropical weathering of the Barama-Mazaruni greenstone belt at Omai gold mine, Guiana Shield. *Applied Geochem.*, 17: 321-336.
- Watong, G.A., R. Kitagawa, Takenos, F.M. Tchoua and D. Njopwouo, 1996. Morphological transformation of kaolin minerals from granite saprolite in the western part of Cameroon. *Clay Sci.*, 1: 67-81.
- Wronkiewicz, D.J. and K.C. Condie, 1987. Geochemistry of Archean shales from the Witwatersrand Supergroup, South Africa: source-area weathering and provenance. *Geochim. Cosmochim. Acta*, 51: 2401-2416.